An Iterative Algorithm for Objective Wind Field Analysis

C. Y. LIU AND W. R. GOODIN[1]

Department of Mechanics and Structures, University of California, Los Angeles 90024

(Manuscript received 21 June 1975, in revised form 25 November 1975)

ABSTRACT

A wind field interpolated from a limited supply of observed data often implies a specific field of divergence, or a violation of the conservation of mass. To minimize the divergence, various objective analyses have been proposed. Three different methods of analysis are investigated and compared with respect to the degree of minimization of wind divergence and the accuracy of wind data at a measured station. The methods are a variational formulation in which the residual error in the continuity equation is minimized, a fixed-vorticity technique, and the presently proposed algorithm in which the measured winds are held fixed while winds at adjacent points are adjusted in order to reduce the divergence. The reduction of wind divergence and the convergence of the iterative scheme are examined. Results of the objective wind field analysis at times depend on subjective judgment in selecting the appropriate initialization algorithm especially for regions with scattered stations.

1. Introduction

Wind prediction is an important task in weather forecasting, for which a complete initial wind distribution must be provided at all grid points in the field of interest. Integration of the model equations can then proceed with, hopefully, a minimum amount of initial errors. Meteorological studies of the jet stream, clear air turbulence, and urban heat islands also require the knowledge of regional wind profiles. In air pollution modeling, the most important meteorological factor affecting the transport of contaminants is the wind. Transport of contaminants by advection exceeds horizontal diffusion by two orders of magnitude on a typical day.[2] Knowledge of the local wind field thus becomes quite important. Regional wind field information is gained from either the prediction of a forecasting model, or more frequently, observed data gathered at various stations.

Wind data as well as other meteorological quantities, such as pressure, can be analyzed subjectively by drawing isopleths, through which irregularities, observational errors, and minor fluctuations are minimized. The reliability of such a subjective analysis is open to personal interpretations, and it is often benefitted by experience. Objective methods are often more desirable as the amount of observed data and the scale of computational machinery increases. Panofsky (1949), who pioneered the method of objective analysis, introduced polynomials to fit pressure data; Gilchrist and Cressman (1954) refined the polynomial representation through the method of least squares. Pressure, generally observed with a higher degree of accuracy then wind vectors, perhaps is more suitable to a polynomial fitting since less "smoothing" is required. An iterative technique through which the divergence of the wind field was minimized while the field of vorticity was retained, was proposed by Endlich (1967). Recently, Dickerson (1973) implemented Sasaki's (1970) variational formulation to generate a divergence-free wind field from observed data acquired in the San Francisco Bay area.

In the present study, as part of an air pollution modeling effort, we propose an iterative algorithm by which a divergence-free wind field is obtained objectively while constraining the wind vectors at observed stations. Results of the present investigation are compared with those of the variational method and a fixed-vorticity scheme. Convergence of the present scheme and its dependence on initial conditions are also examined.

2. Existing wind-smoothing algorithms

Dickerson's algorithm, based on the variational formulation of Sasaki, adopts the vertically integrated continuity equation as the governing equation:

$$\frac{\partial h}{\partial t}+\frac{\partial (uh)}{\partial x}+\frac{\partial (vh)}{\partial y}=0. \tag{1}$$

[1] Present affiliation: Environmental Quality Laboratory, California Institute of Technology, Pasadena, Calif. 91125.

[2] Considering the distribution of carbon monoxide in the Los Angeles basin as illustration, we find that the advective term in the species continuity equation is of the order 10^{-2} ppm s^{-1}, while the corresponding diffusion term is of the order 10^{-4} ppm s^{-1}.

Here h is the height of the inversion base above the topography, or equivalently, the mixing depth; u and v are the x and y velocity components respectively; and t denotes time. When the observed values (signified by subscript o) of u, v and h are used in (1), a nonzero residual error ϵ appears on the right-hand side:

$$\frac{\partial h_o}{\partial t}+\frac{\partial (u_o h_o)}{\partial x}+\frac{\partial (v_o h_o)}{\partial y}=\epsilon. \tag{2}$$

The goal of objective analysis is to obtain a wind field description in which the residual error ϵ is minimized, if not completely removed. In Sasaki's formulation, the requirement that ϵ should be identically equal to zero is called the "strong constraint," that ϵ should be approximately equal to zero is the "weak constraint." The former method is adopted in the present study for comparison. Under the strong constraint, Sasaki found in his variational formulation that a Lagrangian multiplier λ should obey the equation

$$\nabla^2\lambda=-\left[\frac{\partial h_o}{\partial t}+\frac{\partial (u_o h_o)}{\partial x}+\frac{\partial (v_o h_o)}{\partial y}\right], \tag{3}$$

with λ vanishing at all boundaries in the domain of computation. After λ is determined by solving (3), the adjusted values of uh and vh are obtained from the following expressions:

$$\left.\begin{aligned} uh&=u_o h_o+\frac{\partial \lambda}{\partial x}\\ vh&=v_o h_o+\frac{\partial \lambda}{\partial y}\end{aligned}\right\}. \tag{4}$$

Though Eq. (3) for λ is a formal result from Sasaki's analysis, we may, however, interpret λ as a velocity potential corresponding to a mass-source distribution, $-\epsilon$. Hence, the velocity adjustments $\partial\lambda/\partial x$ and $\partial\lambda/\partial y$ should be added to the velocity components u and v respectively [Eqs. (4)]. Dickerson applied the preceding "strong constraint" formulation, as well as the "weak constraint" to the determination of a wind field in the San Francisco area.[3]

The iterative method of Endlich minimized the divergence of the wind field while retaining the vorticity distribution of a desired pattern. He conjectured that such a pattern of vorticity might come from a global forecasting model, or it might be indicated by a rotational pattern in a satellite cloud photograph. A point-by-point iteration, analogous to the Gauss-Seidel method, was adopted by Endlich; its convergence was illustrated by several numerical experiments in lieu of mathematical formalism.

For comparison, we also construct a fixed-vorticity wind field from the same set of initial conditions. The fixed-vorticity wind field herein is obtained from the streamfunction $\psi(x,y,t)$ and vorticity $\zeta(x,y,t)$. Through their definitions, the streamfunction and vorticity are related by an elliptical differential equation

$$\nabla^2\psi=-\zeta. \tag{5}$$

For a given distribution of vorticity ζ, the streamfunction ψ can be obtained by solving (5), provided that appropriate boundary conditions are prescribed at all boundaries. The resutling ψ distribution yields the velocity components u and v:

$$uh=\frac{\partial \psi}{\partial y} \quad \text{and} \quad vh=-\frac{\partial \psi}{\partial x}. \tag{6}$$

The existence of the streamfunction ψ, by definition, affirms the divergence-free nature of the wind kinematics. The appropriate boundary conditions imposed in this algorithm is, in practice, a source of difficulties, since the gradients of ψ are required at the boundary of the computational domain where least data are available.

3. Present method

The two existing techniques, though they might reduce the wind divergence, produce wind vectors substantially different from the observed values. Thus, the computed wind field might have no resemblance to the real wind distribution. To remedy this situation, the variational formalism would have to include additional constraints, which in turn would make the analysis prohibitively complex; or, in the second algorithm, the notion of a fixed pattern of vorticity must be replaced. An iterative algorithm, similar to Endlich's procedure for treating a macroscale wind field, is proposed herein to minimize the divergence while retaining the observed wind vectors.

Consider a quasi-stationary wind field where the time rate of change of the inversion base is small in relation to other spatial variations, namely, $\partial h/\partial t$ may be excluded from the continuity equation (1).[4] The divergence D of the wind field is then

$$\frac{\partial (uh)}{\partial x}+\frac{\partial (vh)}{\partial y}=D. \tag{7}$$

[3] Private communication. The "strong constraint" algorithm has recently been modified by Dickerson to include a vertical velocity component and a revised set of boundary conditions for regions where the local topographical elevations protrude through the base of inversion. Wind vectors at observed stations, however, are free to alter.

[4] There is no conceptual or operational difficulty in the inclusion of $\partial h/\partial t$ in the present analysis. The magnitude of $\partial h/\partial t$, as evaluated from (24), is indeed quite small in comparison with terms in (7).

The volumetric fluxes per unit length, uh and vh, always appear together. Determination of the wind components would require some knowledge of the inversion base h, which may at times be constant in flat terrain, or may have diurnal characteristics in a coastal basin. In any event, the value of h is presumed known. At a grid point (p,q), the simplest finite difference approximation of (7) can be written as

$$D^n_{p,q}=(u^n_{p+1,q}h_{p+1,q}-u^n_{p-1,q}h_{p-1,q})/2\Delta x + (v^n_{p,q+1}h_{p,q+1}-v^n_{p,q-1}h_{p,q-1})/2\Delta y. \quad (8)$$

The superscript n denotes the value of a quantity at the nth iteration; the grid sizes Δx and Δy are assumed constant throughout the domain of computation. To remove the divergence at grid point (p,q), adjustments are made to the u components at $(p-1,q)$ and $(p+1,q)$ grid points. These adjustments to u are equal and of opposite sign. Similar adjustments are made to v at $(p, q+1)$ and $(p, q-1)$ grid points. However, adjustments made at these four points surrounding (p,q) would, in turn, alter the divergence at adjacent points. Thus, the whole grid must be scanned iteratively in order to uniformly reduce the divergence at all locations. The velocities at the $(n+1)$th iteration will be the values at the nth iteration together with the velocity adjustments $\tilde{u}^n_{p,q}$ and $\tilde{v}^n_{p,q}$. In other words, we have

$$\left.\begin{aligned} u^{n+1}_{p+1,q}&=u^n_{p+1,q}+f_{p+1,q}\tilde{u}^n_{p,q}h_{p+1,q}\\ u^{n+1}_{p-1,q}&=u^n_{p-1,q}-f_{p-1,q}\tilde{u}^n_{p,q}h_{p-1,q}\\ v^{n+1}_{p,q+1}&=v^n_{p,q+1}+f_{p,q+1}\tilde{v}^n_{p,q}h_{p,q+1}\\ v^{n+1}_{p,q-1}&=v^n_{p,q-1}-f_{p,q-1}\tilde{v}^n_{p,q}h_{p,q-1}\end{aligned}\right\}. \quad (9)$$

Here the parameter $f_{p,q}$, defined to indicate whether the grid point (p,q) is the location of a wind station, assumes the value of zero at a station and unity at a non-station. Substitution of (9) into (8) yields

$$(f_{p+1,q}+f_{p-1,q})\tilde{u}^n_{p,q}/2\Delta x + (f_{p,q+1}+f_{p,q-1})\tilde{v}^n_{p,q}/2\Delta y+D^n_{p,q}=0. \quad (10)$$

If the first two terms in (10) are assumed to contribute equally to the divergence $D^n_{p,q}$, we find

$$\left.\begin{aligned} \tilde{u}^n_{p,q}&=-D^n_{p,q}\Delta x/(f_{p+1,q}+f_{p-1,q})\\ \tilde{v}^n_{p,q}&=-D^n_{p,q}\Delta y/(f_{p,q+1}+f_{p,q-1})\end{aligned}\right\}. \quad (11)$$

Thus, the solution procedure is as follows. The divergence $D^n_{p,q}$ at the nth iteration is first calculated from (8), $\tilde{u}^n_{p,q}$ and $\tilde{v}^n_{p,q}$ are then computed using (11), and finally the values of $u^{n+1}_{p,q}$ and $v^{n+1}_{p,q}$ are obtained by (9). This procedure is repeated until the divergence is less than a specified value. At the boundary, the velocity components must be prescribed.

This formalism is neither restricted to a four-point finite difference scheme to represent the divergence $D^n_{p,q}$ [Eq. (8)], nor confined to the usage of the immediately adjacent points to carry the full weight of the adjustments at one iteration [Eq. (9)]. In general, the accuracy of the finite difference approximations and the weighting of of $\tilde{u}^n_{p,q}$ on $u^n_{p,q}$ may be altered. Eq. (8) can be rewritten to include the values of u and v at eight grid points;

$$\begin{aligned} D^n_{p,q}=&\,c(u^n_{p+1,q}h_{p+1,q}-u^n_{p-1,q}h_{p-1,q})/2\Delta x\\ &+(1-c)(u^n_{p+2,q}h_{p+2,q}-u^n_{p-2,q}h_{p-2,q})/4\Delta x\\ &+c(v^n_{p,q+1}h_{p,q+1}-v^n_{p,q-1}h_{p,q-1})/2\Delta y\\ &+(1-c)(v^n_{p,q+2}h_{p,q+2}-v^n_{p,q-2}h_{p,q-2})/4\Delta y. \end{aligned} \quad (12)$$

Equation (12) is reduced to the four-point approximation when the parameter c assumes the value of unity; Eq. (12) represents a fourth-order accurate scheme when $c=2/3$. Introduction of the weighting parameters α and β gives

$$u^{n+1}_{p+1,q}=u^n_{p+1,q}+\alpha f_{p+1,q}\tilde{u}^n_{p,q}/h_{p+1,q}, \text{ etc.}, \quad (13)$$

analogous to (9), and

$$u^{n+1}_{p+2,q}=u^n_{p+2,q}+\beta f_{p+2,q}\tilde{u}^n_{p,q}/h_{p+2,q}, \text{ etc.} \quad (14)$$

Clearly $\alpha=1$ and $\beta=0$ would reduce the 8-point system to the 4-point representation previously discussed. With the inclusion of c, α and β, the velocity adjustments $\tilde{u}^n_{p,q}$ and $\tilde{v}^n_{p,q}$ become

$$\left.\begin{aligned} \tilde{u}^n_{p,q}=&-2D^n_{p,q}\Delta x/[c\alpha(f_{p+1,q}+f_{p-1,q}+f_{p,q+1}+f_{p,q-1})\\ &+\tfrac{1}{2}(1-c)\beta(f_{p+2,q}+f_{p-2,q}+f_{p,q+2}+f_{p,q-2})]\\ \tilde{v}^n_{p,q}=&-2D^n_{p,q}\Delta y/[c\alpha(f_{p+1,q}+f_{p-1,q}+f_{p,q+1}+f_{p,q-1})\\ &+\tfrac{1}{2}(1-c)\beta(f_{p+2,q}+f_{p-2,q}+f_{p,q+2}+f_{p,q-2})]\end{aligned}\right\}. \quad (15)$$

The solution procedure in this more general case is exactly the same as before. The success of this iterative procedure hinges on the systematical reduction of the divergence, $D^n_{p,q}$, and the convergence of $u^n_{p,q}$, $v^n_{p,q}$ as n increases.

To examine the reduction of $D^n_{p,q}$, we shall, for simplicity, consider that all $f_{p,q}$ assume the value of unity. Substitution of (15) into (12) gives the value of the divergence at the $(n+1)$th iteration:

$$\begin{aligned} D^{n+1}_{p,q}&=(1-\alpha)D^n_{p,q}\\ &=(1-\alpha)^nD^0_{p,q}. \end{aligned} \quad (16)$$

The change in $D^n_{p,q}$ is independent of the parameters c

and β, and its reduction from the initial value $D^0_{p,q}$ requires that

$$\alpha \leqslant 1. \tag{17}$$

The closer the value of α to unity, the smaller the number of iterations would be required to reduce $D^n_{p,q}$ to satisfy a specific criterion.

Without losing generality, the convergence of the iterative scheme on $u^n_{p,q}$ and $v^n_{p,q}$ may be discussed for a uniform mixing height, namely, $h_{p,q}$= constant. Then the velocity adjustment, $\tilde{u}^n_{p,q}$, through which one-half of the existing $\alpha D^n_{p,q}$ is to be reduced, can be written as

$$\begin{aligned}
&\frac{c}{2}(u^{n+1}_{p+1,q}-u^{n+1}_{p-1,q})+\frac{1-c}{4}(u^{n+1}_{p+2,q}-u^{n+1}_{p-2,q})\\
&\quad=\frac{c}{2}\left(1-\frac{\alpha}{2}\right)(u^n_{p+1,q}-u^n_{p-1,q})+\frac{(1-c)(1-\alpha/2)}{4}\\
&\quad\times(u^n_{p+q,2}-u^n_{p-2,q})-\frac{c\alpha}{4}(v^n_{p,q+1}-v^n_{p,q-1})\frac{\Delta x}{\Delta y}\\
&\qquad-\frac{\alpha(1-c)}{8}(v^n_{p,q+2}-v^n_{p,q-2})\frac{\Delta x}{\Delta y}.
\end{aligned} \tag{18}$$

It is again noteworthy that β does not appear in the preceding equation. In theory, we may consider the distribution of u to be represented by a double Fourier expansion, namely,

$$\text{thus,}\quad \left.\begin{aligned} u^n_{p,q}&=\sum_{p,q} A_{pq}e^{i(p\Delta x+q\Delta y)};\\ u^{n+1}_{p,q}&=\sum_{p,q}\bar{A}_{pq}e^{i(p\Delta x+q\Delta y)}.\end{aligned}\right\} \tag{19}$$

The overbar denotes Fourier coefficients at the $(n+1)$th iteration. Similarly, the other velocity component v can be written as

$$\text{then,}\quad \left.\begin{aligned} v^n_{p,q}&=\sum_{p,q} B_{pq}e^{i(p\Delta x+q\Delta y)};\\ v^{n+1}_{p,q}&=\sum_{p,q}\bar{B}_{pq}e^{i(p\Delta x+q\Delta y)}.\end{aligned}\right\} \tag{20}$$

Substituting (19) into (18) and rearranging, we find

$$\bar{A}_{pq}=\left(1-\frac{\alpha}{2}\right)A_{pq}-\frac{\alpha}{2}\frac{\Delta x}{\Delta y}\left\{\frac{\sin(q\Delta y)+\dfrac{1-c}{2c}\sin(2q\Delta y)}{\sin(p\Delta x)+\dfrac{1-c}{2c}\sin(2p\Delta x)}\right\}. \tag{21}$$

The identical procedure with (20) and (18) for the velocity adjustment $v^n_{p,q}$ leads to a similar expression,

$$\bar{B}_{pq}=-\frac{\alpha}{2}\frac{\Delta x}{\Delta y}\left\{\frac{\sin(p\Delta y)+\dfrac{1-c}{2c}\sin(2p\Delta x)}{\sin(q\Delta y)+\dfrac{1-c}{2c}\sin(2q\Delta y)}\right\}A_{pq}+\left(1-\frac{\alpha}{2}\right)B_{pq}. \tag{22}$$

Equations (21) and (22) can be combined into an amplification matrix $\mathbf{G}$:

$$\begin{pmatrix}\bar{A}_{pq}\\ \bar{B}_{pq}\end{pmatrix}=[\mathbf{G}]\begin{pmatrix}A_{pq}\\ B_{pq}\end{pmatrix},$$

with

$$[\mathbf{G}]=\begin{bmatrix}\dfrac{1-\alpha}{2} & -\dfrac{\alpha}{2}\dfrac{\Delta x}{\Delta y}\left\{\dfrac{\sin(q\Delta y)+\frac{1-c}{2c}\sin(2q\Delta y)}{\sin(p\Delta x)+\frac{1-c}{2c}\sin(2p\Delta x)}\right\}\\ -\dfrac{\alpha}{2}\dfrac{\Delta y}{\Delta x}\left\{\dfrac{\sin(p\Delta x)+\frac{1-c}{2c}\sin(2p\Delta x)}{\sin(q\Delta y)+\frac{1-c}{2c}\sin(2q\Delta y)}\right\} & \dfrac{1-\alpha}{2}\end{bmatrix}.$$

To assure convergence for $u^n_{p,q}$ and $v^n_{p,q}$, we must have $\det[\mathbf{G}]\leqslant 1$, namely,

$$\left|\left(1-\frac{\alpha}{2}\right)^2-\frac{\alpha^2}{4}\right|\leqslant 1,$$

or

$$0\leqslant\alpha\leqslant 2. \tag{23}$$

Equation (23) together with (17) lead to the requirement that the value of α must be equal to or less than unity in order to assure a symmetrical reduction of the divergence and the convergence of the iterative wind velocities. Though c and β do not enter to the aforementioned criterion explicitly, they do, however, affect the magnitude of the divergence as well as that of the wind components, as can be seen in the following section. The usefulness of the present method is better illustrated through its applications.

4. Results

To examine the present iterative algorithm for wind field analysis, we must provide ourselves with observed wind data at scattered stations and the variation of the inversion base h. Using the wind data in Los Angeles

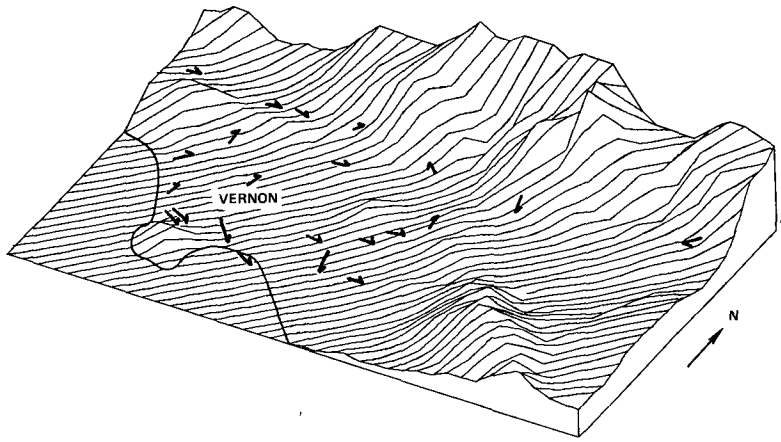

FIG. 1. Measured station velocities, 1500 PST 5 January 1972
Los Angeles Basin, view from southeast.

basin on 5 January 1972 at 1500 PST as an illustration, we cover the region of computation by a 40×25 grid, with each square 2 mi on a side. The measured wind vectors at 22 stations in the basin are shown in Fig. 1.[5]

The diurnal variation of the inversion base h correlated by Neiburger (1974)[6] is separated into two components: one due to solar heating at the surface (HQ) and a second due to wind field divergence (HD). In other words,

$$h = h_0 + \mathrm{HQ} + \mathrm{HD} - (H_{\mathrm{TOPO}} - H_{\mathrm{BASE}}), \qquad (24)$$

where:

h_0	the reference height (Fig. 2)
HQ	$= (\mathrm{HQ})_0 \sin(\pi t/\tau_H + \phi_1) \sin(\pi S/L)$,
HD	$= (\mathrm{HD})_0 \sin(2\pi t/\tau + \phi_2)$,
$(\mathrm{HQ})_0$	the amplitude of heating oscillation, about 400 m in Los Angeles
$(\mathrm{HD})_0$	the amplitude of divergence oscillation, about 60 m
ϕ_1	the phase shift that produces maximum h inland at 1400 PST
ϕ_2	the phase shift that produces maximum h at coast at 0800 PST
S	distance to the nearest coast line
L	the length scale, it is taken to be 120 km
τ_H	the heating period, 12 h
τ	the diurnal period, 24 h
H_{TOPO}	the height of the actual land above sea level
H_{BASE}	the height of coastal plane above sea level, a linear function of the distance S.

Neiburger's correlation, supposedly valid for the entire year, is compared with the observations of Edinger (1973) in Fig. 3 for three different hours on three consecutive days in June of 1970. The graphs in Fig. 3, showing a transect from Santa Monica to Azusa, confirm the expected agreement despite the very simple sinusoidal approximations. Our numerical experiment can then proceed with the values of h as given by (24).

At the outset, the wind field at all grid points must be initialized. There are various arbitrary means available. For instance, the wind vector at a grid point could be computed using a weighted average of all stations within a given radius (12 km in the present application). If the circle with such a radius contains fewer than a specific number of stations (say, five), then it is expanded until it does. In the present examples, the weighting function is the inverse radius squared. At the other extreme one may simply impose the wind vector at the nearest station as the initial values at a grid point. The dependence of the final result on initial conditions is to be examined further.

With the same set of initial conditions, three different algorithms for objective wind field analysis were examined: Dickerson-Sasaki's "strong constraint" algorithm, a fixed-vorticity algorithm, and the present fixed-station-velocity algorithm. In Dickerson-Sasaki's scheme, the elliptical differential equation [Eq. (3)] is solved iteratively using a 9-point relaxation procedure studied by Wurtele and Clark (1965). The same method is applied to solve the streamfunction equation [Eq. (5)] for the fixed-vorticity algorithm. Results of all three schemes are given in Figs. 4–6. Qualitatively, the

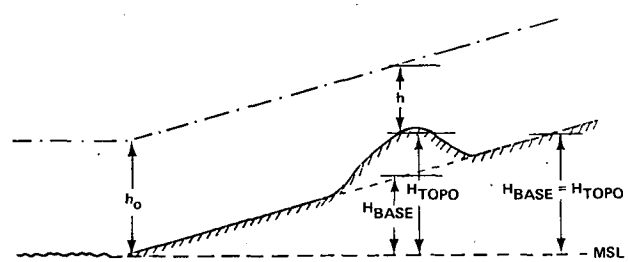

FIG. 2. Nomenclature used for inversion base calculation.

[5] The grid point nearest to an observed station assumes the wind vectors of that station. An interpolation scheme can be readily devised, if the grid sizes become large.

[6] Private communication.

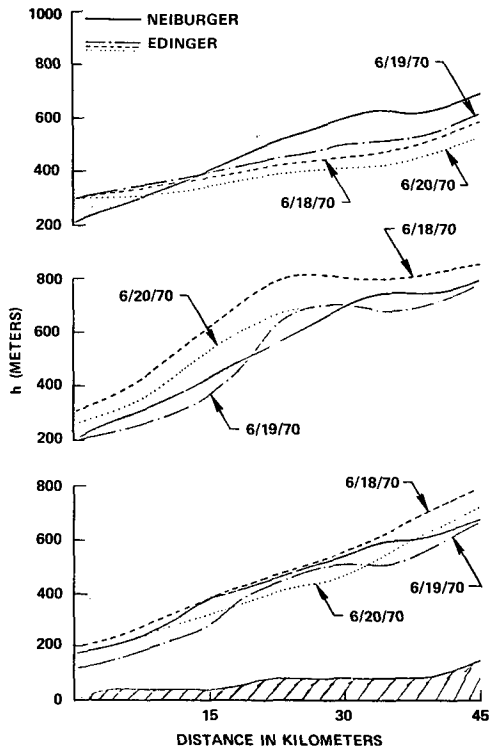

FIG. 3. Comparison of calculated and measured inversion bases at 1500 PST (bottom), 1200 PST (middle), 0900 PST (top).

"strong constraint" algorithm yields a wind field (Fig. 4) showing a sea breeze heading inland almost uniformly; a similar observation can be made about the fixed-vorticity algorithm (Fig. 5). In comparison with Fig. 1, one observes that wind vectors at various locations in Figs. 4–5 have little resemblance to their observed values. The fixed-velocity algorithm gives a wind field (Fig. 6) considerably more complex than a unidirectional sea breeze, particularly in the downtown Los Angeles area. Quantitatively, the wind divergence can be characterized by its mean-square divergence, defined as $[10^{-3}\sum_{p,q}(D^n_{p,q})^2]^{\frac{1}{2}}$. Its starting value of order unity (per second) practically remains the same after 200 iterations by the "strong constraint" algorithm (Fig. 7). The fixed-vorticity algorithm indeed reduces the divergence to an exceedingly low value, $O(10^{-6}\ s^{-1})$, as shown in Fig. 7. A further reduction of the mean-squared divergence would not be meaningful, as the computer employed here has only a seven-digit word length. Accuracy of the present algorithm, as illustrated by a 4-point differencing scheme ($c=1$, $\beta=0$) and an 8-point differencing scheme ($c=2/3$, $\beta=1/3$), is shown by the reduction of the mean-square divergence from its initial value to the order of $10^{-3}\ s^{-1}$ or $10^{-4}\ s^{-1}$. Again, the merit of further iteration beyond $n=250$ is dubious, as the improved accuracy becomes comparable to round-off errors. With the exception of the "strong constraint" algorithm, both the fixed-vorticity and the present schemes seem satisfactory in the objective reduction of wind divergence, while the former method yields the "smoothest" wind field of all in such a test.

One early experiment in objective wind field analysis was that of Panofsky, who compared winds observed and winds computed from cubic polynomials for a December day in 1945. Because of the smoothing by the fitted polynomials, the computed winds were much less erratic. If one attempts to predict wind vectors

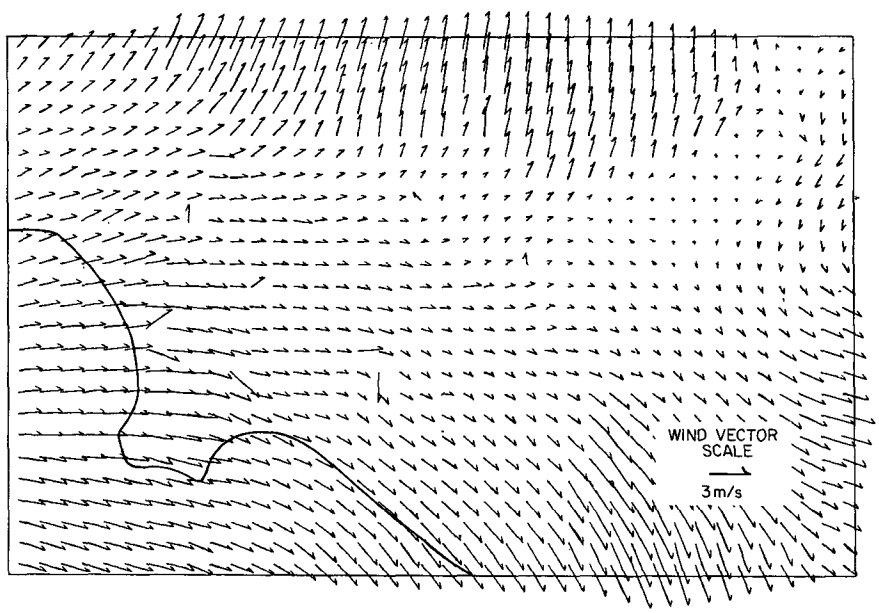

FIG. 4. Wind field produced by Dickerson's algorithm, initialized by weighted-average.

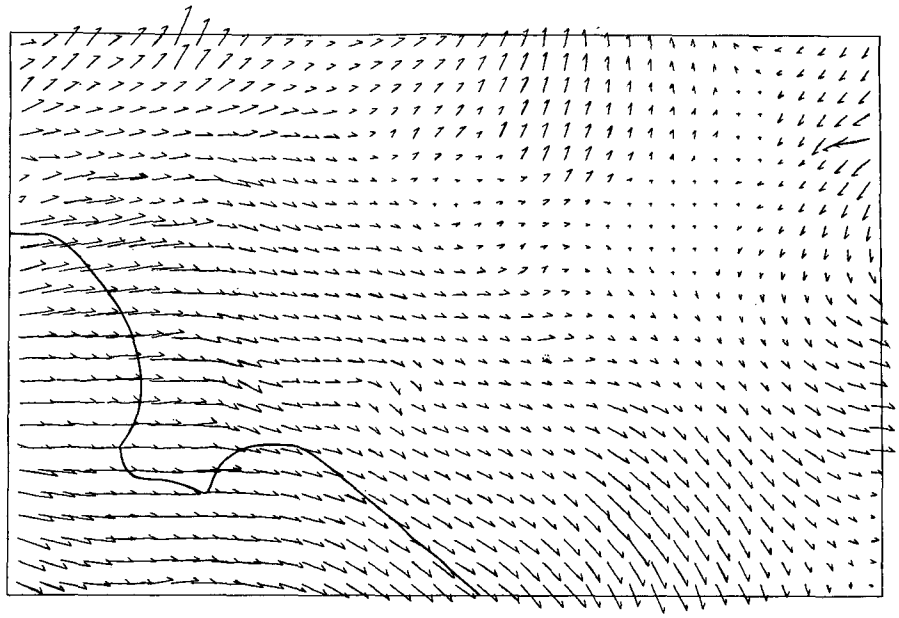

FIG. 5. Wind field produced by fixed-vorticity algorithm, initialized by weighted average.

at observed stations, one would find at times substantial discrepancy between observed and predicted values. The prediction of a wind field by any formulation based on data gathered from finite number of scattered stations is mathematically an ill-posed problem, to which a nonunique solution is expected. Hence the convergence of $u^n_{p,q}$ or $v^n_{p,q}$ in the preceding discussion only signifies convergence in Cauchy's sense, namely, convergence toward some definitive value. The dependence of final results on the subjective initialization requires further examination.

We initialized the present algorithm for 1500 PST 5 January 1972 by 1) the weighted-average scheme and 2) the nearest-station scheme. The wind field shown in Fig. 6 represents the results generated by the weighted-average initialization, while that in Fig. 8 is the product through the nearest-station method. Though the local, as well as the global, divergence by

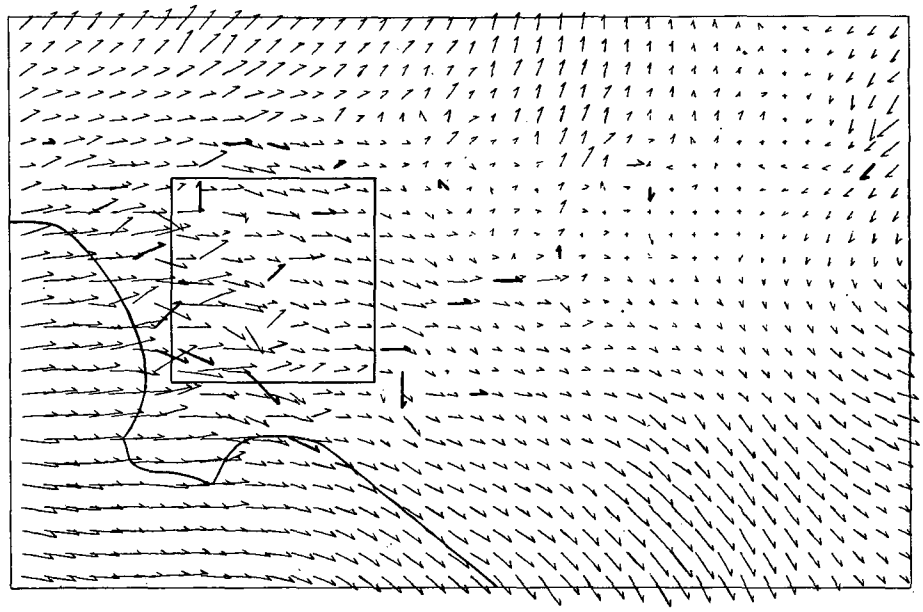

FIG. 6. Wind field produced by fixed-station-velocity algorithm, initialized by weighted average. Heavy-lined wind vectors are observed values.

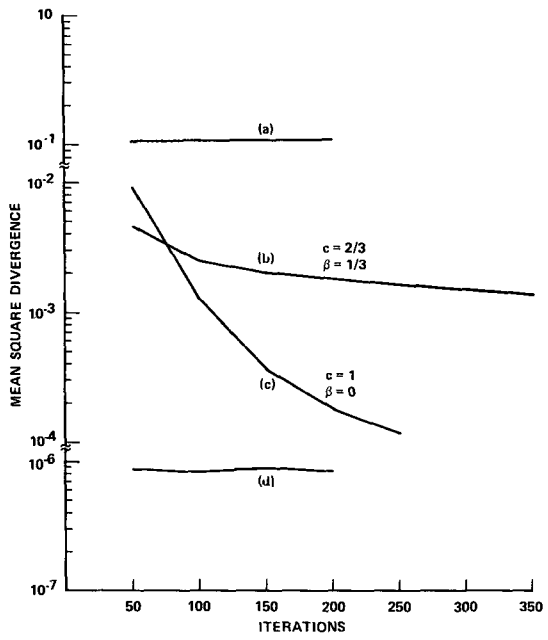

FIG. 7. Mean square divergence for the three algorithms: (a) Sasaki-Dickerson; (b,c) fixed-station-velocity algorithm; (d) fixed-vorticity scheme.

these two different schemes of initialization is of the same order, 10^{-3} s^{-1}, the two wind fields depart substantially in areas where observed station data are sparse or non-existent. In such areas, initialization by assigning the wind vector at the nearest station to a grid point would in effect produce the final result, since a uniform wind field is naturally divergence-free.

To focus on the difference between the observed and the predicted wind vectors at a specified station, we repeat the computations leading to Figs. 6 and 8 by ignoring the wind data at Vernon. The Vernon station is chosen because it is located close to the center of the basin, and it is surrounded by several measuring stations. The predicted wind fields with and without the Vernon data, using both the weighted-average and the nearest-station schemes for initialization, are shown in Fig. 9. The predicted wind direction at the Vernon station differs markedly from its observed value. This is perhaps nor surprising, since Vernon is the last station inland (Fig. 1) showing a northeast sea breeze. Hence, caution must be exercised in interpreting a wind field generated from data gathered from a number of scattered stations. The omission of a key station at times may be crucial to the final results. The present analysis would indeed become quite objective once the scheme for initialization is selected.

5. Summary

Three numerical techniques for objective wind field analysis, i.e., the generation of a divergence-free wind field from a limited supply of observed data, have been compared. The "strong-constraint" algorithm fails to reduce the divergence, and it also fails to hold the station wind vectors reasonably constant. The fixed-vorticity algorithm reduces the divergence significantly; however, wind vectors at stations are altered. The present iterative algorithm, in which the observed winds are held fixed as additional constraints, also reduces the wind divergence successfully. Wind velocities in the iterative algorithm are shown to converge to definite final values,

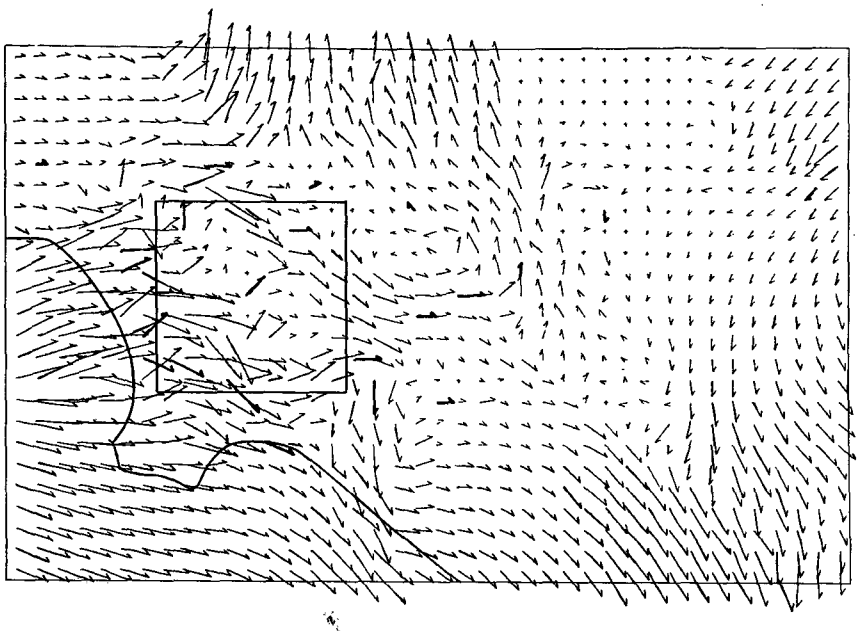

FIG. 8. Fixed-station-velocity algorithm initialized by nearest-station scheme. The central area inside the square is used for testing of initial conditions in Fig. 9.

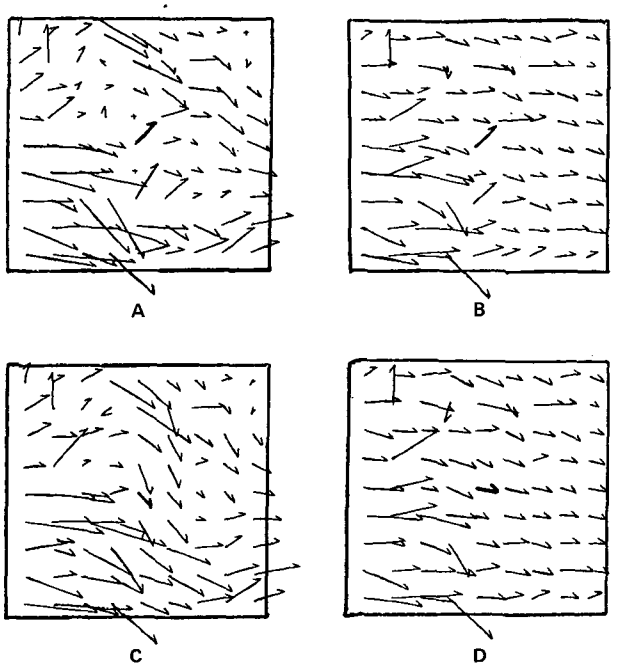

FIG. 9. Comparison of different methods of initialization: (A) nearest-station scheme (Vernon included); (B) weighted-average scheme (Vernon included); (C) nearest-station scheme (Vernon not included); (D) weighted-average scheme (Vernon not included).

and wind divergence is reduced continuously. Wind vectors, particularly those situated in regions with sparsely scattered stations, depend on the scheme of initialization. Under these circumstances, the objective analysis would involve some subjective judgment in selecting the apporpriate initialization scheme. Some physical understanding of the wind field is not only helpful, but mandatory.

Since there are uncertainties in wind measurements, it does not seem desirable to hold the observed values absolutely fixed. A modified version of the present algorithm could be formulated in which one allows the wind-station velocities to vary by a prescribed limit. Such analysis would generate a "smoother" wind field by allowing the amplitude of the short-wavelength components in the Fourier expansion to reduce. The reduction in the spatial gradients of wind components enhances the usefulness of the resulting wind field, which in turn becomes input to weather forecasting equations, or to air pollution models.

Acknowledgments. This study was sponsored by the National Aeronautics and Space Administration, Ames Research Center, under UCL-302. Many helpful suggestions of Dr. Paul Swan are sincerely appreciated.

REFERENCES

Dickerson, M. H., 1973: A mass-consistent wind field model for the San Francisco Bay area. UCRL-74265, Lawrence Livermore Laboratory, Calif.

Edinger, J. G., 1973: Vertical distribution of photochemical smog in the Los Angeles basin. *Environ. Sci. Tech.*, **7**, 247–252.

Endlich, R. M., 1967: An iterative method for altering the kinematic properties of wind fields. *J. Appl. Meteor.*, **6**, 837–844.

Gilchrist, B., and G. P. Cressman, 1954: An experiment in objective analysis. *Tellus*, **6**, 309–318.

Panofsky, H. A., 1949: Objective weather-map analysis. *J. Meteor.*, **6**, 386–392.

Sasaki, Y., 1970: Some basic formalisms in numerical variational analysis. *Mon. Wea. Rev.*, **98**, 875–883.

Wurtele, M. G., and C. Clark, 1965: The relative efficiency of certain schema in the solution of a Poisson equation. *J. Atmos. Sci.*, **22**, 436–439.